Macromolecular Research, Vol. 15, No. 6, pp 560-564 (2007)

Photostabilization and Cure Kinetics of UV-Curable Optical Resins Containing Photostabilizers

Jung-Dae Cho

Institute of Photonics & Surface Treatment, Q-Sys Co. Ltd., Gwangju 500-460, Korea

Sung-Hwa Kim and In-Cheol Chang

Optical Solution Lab., Central R&D Institute, Samsung Electro-mechanics, Suwon 443-743, Korea

Kwon-Seok Kim and Jin-Who Hong*

Department of Polymer Science & Engineering, Chosun University, Gwangju 501-759, Korea

Received May 23, 2007; Revised August 6, 2007

Abstract: The photostabilization and cure kinetics of UV-curable, optical resins containing various formulations of photostabilizers were investigated to determine the system with the highest cure conversion and durability. Photo-DSC analysis revealed that increasing the concentration of a UV absorber (UVA) decreased both the cross-link density and the cure rate due to competition for the incident photons between the photoinitiator and the UVA, whereas including a hindered amine light stabilizer (HALS) hardly affected either the cure conversion or the cure rate due to its very low absorption of 365 nm. This result was confirmed by FTIR-ATR spectroscopy and UV-visible spectroscopy analyses. QUV ageing experiments showed that the cure conversion and durability were the highest for the UVA/ HALS formulation at a ratio of 1 : 2, which is due to their synergistic action.

Keywords: photostabilization, cure kinetics, UV-curable optical resin, photo-DSC, FTIR-ATR.

Introduction

UV-initiated polymerized materials have recently received considerable attention due to their rapid reactivity, environmentally friendly (solvent-free) curing, and the variety of formulations available for applications such as electronics, photonics, coatings, adhesives, dental-restorative materials, varnishes, and inks.[1-3] In electronics-industry applications, UV-curable materials have been widely used in photolithographic fabrication, UV embossing replication processes, and UV nanoimprint lithography processes.[4-9] Many electronics companies competing in the mobile phone market focus on the slimness of these devices so as to enhance their portability. A promising approach is to employ camera modules whose thickness is comparable to that of a display panel, facilitating a new arrangement of the camera module at the rim of the display panel. A proposed wafer-scale camera module was fabricated using a wafer-scale UV embossing replication process in which UV-curable resins formed wafer-scale lenses, which also gave lens designers significant freedom in material selection.[9] However, the durability of UV-cured embossed lenses has not been fully considered in outdoor applications, given that UV solar radiation can cause the photodegradation, discoloration, and a serious decrease in the light transmittance of a UV-cured optical resin.

Introducing a photostabilizer such as a UV absorber (UVA) into the resin formulation not only increases the durability of the cured resin subject to photoageing but also effectively screens UV solar radiation, thus greatly reducing the photodegradation of UV-cured organic materials.[10-12] However, the addition of UVA to the resin formulation is expected to reduce the cure speed due to its filtering the UV radiation. Other photostabilizers such as a hindered amine light stabilizer (HALS) are known to have little effect on the UV curing process whilst having a strong stabilizing effect on the photoinduced degradation. Moreover, the presence of HALS was found to significantly increase the life of the UVA, and thus prolong its screening effect upon weathering.[10]

In order to improve the weathering resistance of UV-cured optical resin, it is important to understand how photostabilizers influence the curing behavior and kinetics within the organic matrix. An accurate kinetics analysis of the systems would help in designing the most appropriate formulation and controlling the curing process. The aim of the present

*Corresponding Author. E-mail: jhhong@chosun.ac.kr

study was to quantify the enhancement of the weathering resistance of UV-cured optical resin obtained by the addition of different types of photostabilizer. The effects of different photostabilizers on both the cure kinetics and the photodegradation process were investigated using photodifferential scanning calorimetry (photo-DSC), Fourier-transform infrared spectroscopy with attenuated total internal reflection (FTIR-ATR) spectroscopy, UV-visible spectroscopy, and a QUV weatherometer, from which the most efficient system was determined with respect to the cure conversion and durability.

Experimental

Materials and Curing Process. UV-curable fluorinated acrylate (ChemOptics) containing a photoinitiator was used as an optical resin since it is well known that photopolymers containing fluorine exhibit good release characteristics, with the resin exhibiting very low shrinkage. The UVA Tinuvin 328 (Ciba Specialty Chemicals) and the HALS Tinuvin 292 (Ciba Specialty Chemicals) were used as photostabilizers. The structures of these compounds are shown in Figure 1, and both were used as received. The liquid formulations were applied to a glass substrate at a thickness of ~100 μm using a wire-wound rod, and the wet films were exposed to UV radiation from a metal halide lamp (EFOS UV System) via a fiberoptic light pipe under an inert atmosphere such as nitrogen. The UV-light intensity at the sample was 14 mW/cm^2 at 365 nm.

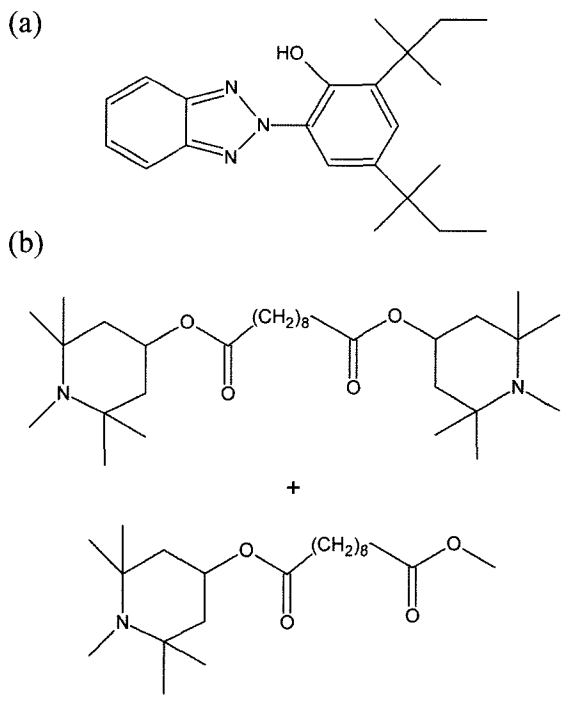

Figure 1. Chemical structures of (a) the UVA (Tinuvin 328) and (b) the HALS (Tinuvin 292) used in this study.

Photo-DSC. The photo-DSC experiments were performed using a differential scanning calorimeter equipped with a photocalorimetric accessory (TA 5000/DPC System). The initiation light source was a 200-W high-pressure mercury lamp, which gave a UV light intensity at the sample of 14 mW/cm^2 at 365 nm. Samples weighing 1.0 ± 0.1 (mean ± SD) mg were placed in uncovered aluminum pans, and a reference aluminum pan was left empty. The exothermic heat achieved for the photocuring at 70 °C was 273 J/g, and was considered as the total heat, ΔH_{total}, for the fully cured resin. This value was used in the subsequent analysis. TA Instruments software was employed to obtain the results from the photo-DSC experiments.

FTIR-ATR Spectroscopy. FTIR-ATR spectra of the samples were recorded on a Perkin-Elmer Spectrum GX device using a horizontal ATR accessory for FTIR spectroscopy (PIKE Technologies), which was continuously purged with purified air that was free of carbon dioxide and water (using a desiccant-based air dryer from New Techniques). To increase the signal-to-noise ratio, each set of reference and sample spectra shown here represents the average of 128 scans recorded at a resolution of 8 cm^{-1}. A ZnSe crystal was used as the internal reflection element, and the incident angle was 45°. The depth of penetration (D_p), which depends on the wavelength (λ), can be calculated from the following equation:[13,14]

$$D_p = \frac{\lambda}{2\pi(n_1^2 \sin^2\theta - n_2^2)^{1/2}} \quad (1)$$

where θ is the angle of incidence, and n_1 and n_2 are the refractive indices of the reflection element and the sample, respectively.

UV-Visible Spectroscopy. The absorption spectra of the photostabilizers (Tinuvin 328 and Tinuvin 292) were obtained using a Cary 3 Bio UV-visible spectrophotometer. Dilutions of 0.01 g/L in methylene chloride were prepared, and quartz cells with a path length of 1.0 cm were used in the analysis.

Photoageing Experiments. Accelerated artificial UV-induced ageing was implemented in a QUV weatherometer (Q-Panel Lab Products) that simulates the damage caused by sunlight, rain, and dew. The UV-cured samples coated onto a glass substrate at a thickness of ~100 μm were mounted on aluminum sample holders and subjected to UV ageing by exposure to UVB-313 fluorescent UV lamps under wet cycle conditions: 8 h of UV irradiation at 70 °C, followed by 4 h of dark condensation at 50°C for up to 2,000 h. The UV light intensity was 0.6 W/m^2 at 313 nm. Yellowness index (YI) was measured by a colorimeter (Chroma Meter CR-300, Minolta) using the CIE $L^*a^*b^*$ system (Commission Internationale de l'Eclairage, 1976), and calculated from the following equation:[17]

$$YI = [(1.28X - 1.06Z)/Y] \times 100 \quad (2)$$

where X, Y, and Z are the tristimulus values. Each reported measurement represents the average value of three measurements.

Results and Discussion

The UV-curable optical resin formulations prepared by adding photostabilizers at various concentrations to the optical resin are listed in Table I. The cure kinetics was investigated using photo-DSC to clarify the photopolymerization process. Photo-DSC experiments are capable of providing kinetics data in which the measured heat flow can be converted directly to the ultimate percentage conversion and polymerization rate for a given amount of formulation, with the obtained data reflecting the overall curing reaction of the sample.[15-19] However, it should be noted that the cure kinetics data used in this study are essentially empirical and do not provide any mechanistic insight.

Figure 2 shows the photo-DSC exotherms for the photopolymerization of the UV-curable optical resin formulations. The amounts of heat released, the ultimate percentage conversions, the peak maxima, and the maximum polymerization rates ($R_{p,max}$) derived from Figure 2 are collected in Table II.

These kinetics data indicated that both the cross-link density (higher exothermic heat and higher percentage conversion mean higher cross-link density) and the cure rate (lower peak maximum and higher $R_{p,max}$ mean faster cure rate) decreased with increasing concentration of the UVA photostabilizer (Tinuvin 328).[1,18] This result is as expected from competition for the incident photons between the photoinitiator and the UVA. In contrast, a quite different behavior was observed in the presence of the HALS photostabilizer (Tinuvin 292): in the case of formulation F (containing only HALS at 1 wt%), there were almost no changes in the kinetics data, indicating that the HALS hardly affected either the cure conversion or the cure rate. This is supported by additional experiments performed using UV-visible spectroscopy. Figure 3 shows the absorption spectra of the photostabilizers in the range 200-500 nm, and indicates that the absorption at 365 nm is high for UVA but very low for HALS, inferring that the HALS does not compete with the photoinitiator for the absorption of incident photons.

Other experiments were designed to obtain some mecha-

Table I. Formulations of UV-Curable Optical Resins Containing Photostabilizers at Various Concentrations. Data Values are weight Percentages

Component	A	B	C	D	E	F
Optical resin[a]	100	100	100	100	100	100
Tinuvin 328[b]	0	1	0.67	0.5	0.33	0
Tinuvin 292[c]	0	0	0.33	0.5	0.67	1

[a]ChemOptics. [b]UVA (Ciba Specialty Chemicals). [c]HALS (Ciba Specialty Chemicals).

Table II. Exotherm Data Obtained by Photo-DSC on the Photopolymerization of the Formulations Listed in Table I

Formulation	ΔH (J/g)	Conversion (%)	Peak Maximum (min)	$R_{p,max}$[a] (1/min)
A	240	88	0.163	2.21
B	199	74	0.190	1.44
C	207	76	0.186	1.53
D	218	80	0.176	1.79
E	229	84	0.169	2.02
F	235	87	0.163	2.20

[a]$R_{p,max}$: maximum polymerization rate ($R_p = d\alpha/dt$, where α is the fraction of resin converted).

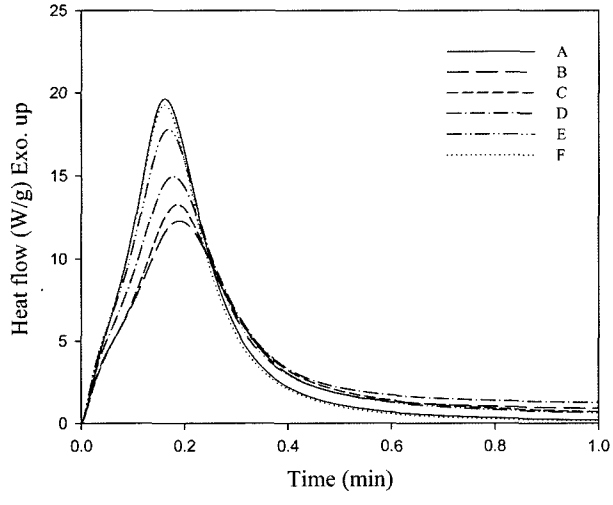

Figure 2. Photo-DSC exotherms for the photopolymerization of UV-curable optical resin formulations A-F at 30 °C. Sample weight: 1.0 mg, light intensity: 35 mW/cm^2 at 365 nm.

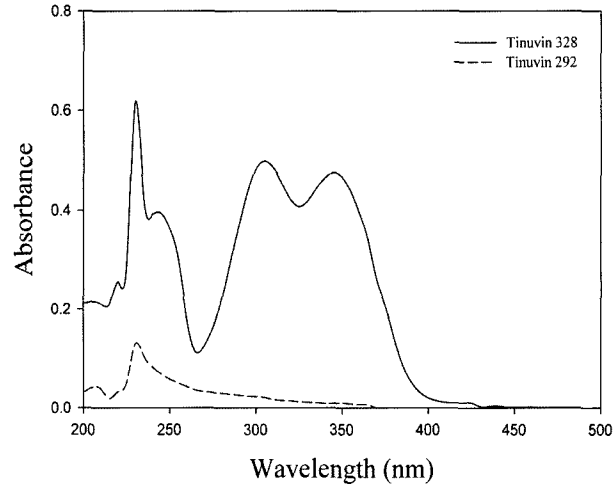

Figure 3. Absorption spectra of Tinuvin 328 (the UVA) and Tinuvin 292 (the HALS).

nistic insight using FTIR-ATR spectroscopy. Figure 4 shows the FTIR-ATR spectra of formulation A according to the UV curing time. The band at 1600 cm^{-1} (due to aromatic stretching vibration of C = C bonds) was used as an internal reference peak since its intensity in the resin was stable during the cross-linking reaction, whereas the band at 810 cm^{-1} (due to deformation modes of the = CH acryl group) was also used to quantify the extent of cure because the prevalence of this band decreases as the cure reaction proceeds. The FTIR-ATR relative intensity ratios of these two bands (810 cm^{-1}/1600 cm^{-1}) of formulations A-F after 60 s of UV curing are presented in Figure 5, which reveals that the extent of the cure reaction decreased as the concentration of UVA increased, but was hardly affected by HALS. This experimental observation is consistent with the photo-DSC

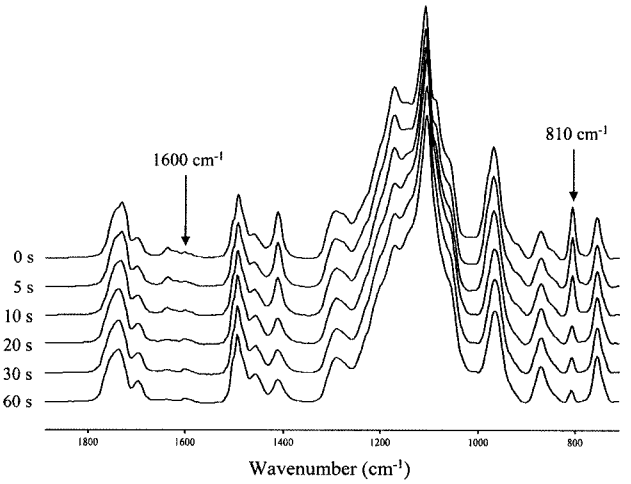

Figure 4. FTIR-ATR spectra of formulation A according to the UV curing time. Sample thickness: ~100 μm, light intensity: 14 mW/cm^2 at 365 nm.

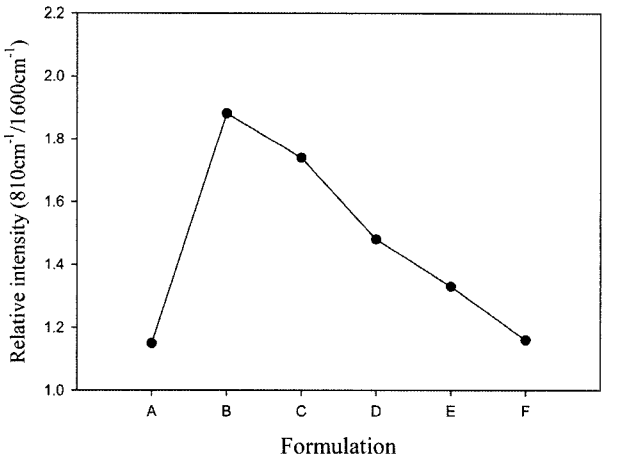

Figure 5. FTIR-ATR relative intensity ratios of formulations A-F after 60 s of UV curing.

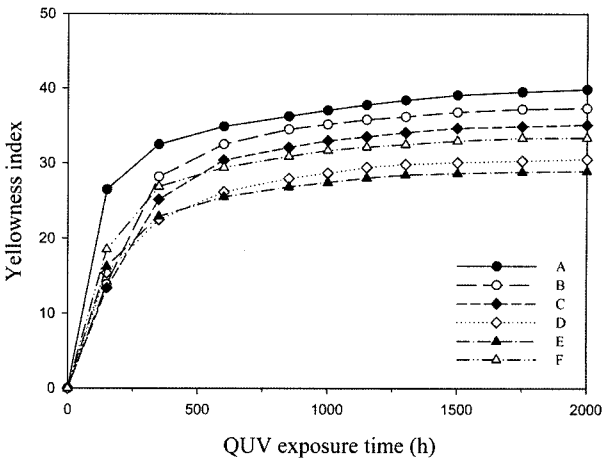

Figure 6. Changes in the yellowing index of formulations A-F subject to QUV ageing.

experimental results.

The weathering resistance of the UV-cured optical resins was evaluated by monitoring the yellowing occurring upon continuous exposure to fluorescent lamps in a QUV weatherometer. The changes in the yellowing index of the formulations subject to QUV ageing are shown in Figure 6, which indicates that the weather resistance was higher for formulations with photostabilizers (B-F) than for that without photostabilizer (A). Comparing the results for formulations B-F, it is noteworthy that before 200 h of QUV ageing (i.e., the initial UV exposure stage), the yellowness index decreased with an increasing concentration of UVA, which implies that the UVA effectively photostabilized the UV-cured optical resins. However, the opposite results were observed after 500 h of QUV ageing. This may be attributable to incomplete cure conversion due to internal filtering by the UVA during the curing process (Table II) resulting in many unreacted double-bond molecules remaining in the organic matrix after UV curing, with these molecules accelerating the yellowing of the UV-cured optical resin.

The presence of the HALS significantly increases the life of the UVA, and thus will prolong its screening effect upon weathering.[10] Formulation D (containing equal amounts of UVA and HALS) exhibited a good resistance to photodegradation. However, the best photostabilization and the highest cure conversion and durability were obtained with formulation E (UVA and HALS at a ratio of 1 : 2).

Conclusions

Photo-DSC, UV-visible spectroscopy, FTIR-ATR spectroscopy, and a QUV weatherometer have been used to investigate the photostabilization and cure kinetics of UV-curable optical resins containing photostabilizers in order to determine the system with the highest cure conversion and dura-

bility. Photo-DSC analysis revealed that increasing the concentration of UVA decreased both the cross-link density and the cure rate, which was due to competition for the incident photons between the photoinitiator and the UVA, whereas the HALS had little affect on either the cure conversion or the cure rate due to it exhibiting little absorption at 365 nm. This result was confirmed by FTIR-ATR spectroscopy and UV-visible spectroscopy analyses. The QUV ageing experiments showed that the cure conversion and durability were highest in the UV-curable optical resin with UVA and HALS at a ratio of 1 : 2 due to their synergistic action in which the presence of HALS significantly increased the life time of the UVA, subsequently prolong its screening effect upon weathering.

Acknowledgement. This study was supported by research funds from Chosun University in 2005.

References

(1) P. K. T. Oldring, *Chemistry & Technology of UV & EB Formulation for Coatings Inks & Paints*, Vols. 1-4, SITA Technology, London, 1991.
(2) A. Reiser, *Photoreactive Polymers*, Wiley, New York, 1989.
(3) C. G. Roffey, *Photopolymerization of Surface Coatings*, Wiley, New York, 1982.
(4) L. Dellmann, S. Roth, C. Beuret, L. Paratte, G.-A. Racine, H. Lorenz, M. Despont, P. Renaud, P. Vettiger, and N. de Rooij, *Microsyst. Technol.*, **4**, 147 (1998).
(5) V. Seidemann, S. Bütefisch, and S. Büttgenbach, *Sens. Actuators A: Phys.*, **97-98**, 457 (2002).
(6) T. Kyu, S. Meng, H. Duran, K. Nanjundiah, and G. R. Yandek, *Macromol. Res.*, **14**, 155 (2006).
(7) S. H. Nam, J. W. Kang, and J. J. Kim, *Macromol. Res.*, **14**, 114 (2006).
(8) Y. Hirai, S. Harada, S. Isaka, M. Kobayashi, and Y. Tanaka, *Jpn. J. Appl. Phys.*, **41**, 4186 (2002).
(9) D. I. Shin, S. H. Kim, H. S. Jeong, S. C. Lee, Y. S. Jin, J. E. Noh, H. R. Oh, K. U. Lee, D. H. Shin, and S. H. Song, *Proceedings of SPIE-IS&T Electronic Imaging*, **6068**, 60680Q-1 (2006).
(10) C. Decker and S. Biry, *Prog. Org. Coat.*, **29**, 81 (1996).
(11) C. Decker and K. Zahouily, *Polym. Degrad. Stab.*, **64**, 293 (1999).
(12) S. Zeren, *Macromol. Symp.*, **187**, 343 (2002).
(13) J. D. Cho, S. G. Kim, and J.W. Hong, *J. Appl. Polym. Sci.*, **99**, 1446 (2006).
(14) J. W. Hong and H. K. Kim, *Macromol. Res.*, **14**, 617 (2006).
(15) S. C. Clark, C. E. Hoyle, S. Jonsson, F. Morel, and C. Decker, *Polymer*, **40**, 5063 (1999).
(16) J. D. Cho, Y. B. Kim, H. T. Ju, and J. W. Hong, *Macromol. Res.*, **13**, 362 (2005).
(17) J. D. Cho, H. K. Kim, Y. S. Kim, and J. W. Hong, *Polym. Test.*, **22**, 633 (2003).
(18) J. D. Cho, H. T. Ju, and J. W. Hong, *J. Polym. Sci.; Part A: Polym. Chem.*, **43**, 658 (2005).
(19) J. D. Cho, H. T. Ju, Y. S. Park, and J. W. Hong, *Macromol. Mater. Eng.*, **291**, 1155 (2006).